International Journal of Science and Research (IJSR)
ISSN: 2319-7064
Impact Factor 2025: 7.089

Graphite-Assisted Copper Electroplated Bilayer Counter Electrodes on Flexible Polyethylene Terephthalate Substrate for High-Efficiency Dye-Sensitized Solar Cells

Ahana Roy[1], Sinjan Roychowdhury[2], Shyamal Datta[3]

[1]Independent Researcher, Shyamal Sir's Tuition, Dankuni, WestBengal-712311, India
Email: *ahanaroy.3d[at]gmail.com*

[1]Independent Researcher, Shyamal Sir's Tuition, Dankuni, WestBengal-712311, India
Email: *roychowdhurysrc23[at]gmail.com*

[1]Independent Researcher, Shyamal Sir's Tuition, Dankuni, WestBengal-712311, India
Corresponding Author Email: *rohitdatta500[at]gmail.com*

Abstract: ***As potential low-cost solar cells for the upcoming generation of photovoltaic technology, Dye-sensitized solar cells (DSSCs) have emerged as a promising alternative for photovoltaic research. The photovoltaic performance with long-term stability is largely influenced by the counter electrode used in the DSSC solar cell. Research on dye-sensitized solar cells has been the main emphasis for replacing costly platinum counter electrodes. A cost-effective, flexible substrate, such as PET coated with a conductive surface, offers a large surface area that facilitates the redox reaction by collecting electrons easily. Herein, we report*** **dye-sensitized solar cells (DSSCs*) based on Graphite assisted with copper electroplated bilayer counter electrodes on polyethylene terephthalate (PET) substrate. A device assembly with a hierarchical architecture, comprising FTO/TiO_2 (ETL)/graphite-assisted electroplated copper, was fabricated for experimental investigation. Natural dyes were extracted from Hibiscus flower in an ethanol medium, which acts as a natural sensitizer in the DSSC. A quasi-solid-state electrolyte prepared with iodide/tri-iodide within a cellulose base medium was employed as redox charge transport medium. The as-prepared sample was characterized using various analytical tools to explore Light absorption properties, surface morphology and structural properties via ultraviolet–visible, field emission scanning electron microscopy, and X-ray diffraction analyses, respectively. Furthermore, the solar cell sample was tested under AM 1.5 G solar illumination to envisage photovoltaic performance. The as-prepared solar device hierarchical architecture, comprising graphite assisted by an electroplated copper layer, shows a PCE of 3%, which is almost 150% higher than that of a graphite counter electrode without a copper layer.***

Keywords: DSSC solar cell, flexible counter electrode, nanomaterial, thin film synthesis

1. Introduction

The world's energy crisis is worsening due to high population growth and the depletion of conventional energy sources like fossil fuels, which are driving up power demand [1]. Finding innovative and alternative sustainable energy sources that are both economically viable and environmentally sustainable is crucial to resolving this dilemma [2]. One of the most promising and optimistic approaches is solar energy, which offers a plentiful, renewable energy source with a small carbon imprint [3]. The efficient conversion of solar irradiation into other forms of energy, such as electrical energy, has been the subject of numerous analytical studies [1-3]. Dye-sensitized solar cells are among the newest solar energy-harvesting technologies that harness sunlight in a very easy way [4]. For almost 20 years, dye-sensitized solar cells (DSSCs), a kind of thin-film solar cell, have been the subject of intensive research because of their versatility and optimized low manufacturing costs [5].

A class of third-generation categorized solar cells known as DSSCs has garnered a lot of research interest because of its enormous potential for flexible and affordable photovoltaic applications [6]. Since their inception in 1991 by Michael Grätzel and Brian O'Regan, DSSCs have gained notable recognition for their effective conversion of solar radiation into electrical energy [7]. In contrast to traditional silicon-based solar cells, DSSCs use organic dye molecules to absorb a wide range of the light spectrum and produce electron hole pair during excitation, which undergo a number of electrochemical reactions to transform into electrical energy [8]. DSSCs' hierarchical structure generally consists of three primary elements: a transparent conductive glass substrate with a Nano crystalline titanium dioxide layer coated with dye, an electrolyte made of an iodide (I^-)/tri-iodide (I_3^-) redox pair dissolved in an organic solvent, and a counter electrode [9]. The counter electrode extracts electrons via an external circuit and facilitates charge transport, which offers both the reduction of the redox electrolyte and the transport of holes in the solid electrolyte.[10] DSSCs operate through the interlinking of a multicomponent hierarchical architecture, which means that enhancing device efficiency requires a multifaceted optimized strategy [11]. The primary light-absorbing element of the DSSC is the dye or photosensitizer, which absorbs energy and creates photo generated charged particles [12]. The dyes are categorized into three groups: natural dyes, organic metal-free dyes, and metal-based dyes. Natural dye originates from sources like chlorophylls, flavonoids, and anthocyanin etc [13]. Inorganic dyes that do not possess metals and are derived from squaraine, coumarin, indoline, phenothiazine, triphenylamine, fluorene, thienopyrazine, carbazole, and tetrahydroquinoline have been

created [14]. These dyes, when used with the DSSC shows satisfactory performance, achieving power conversion efficiencies (PCE) up to 10.3 % [13-14].

Counter electrodes play a crucial role in DSSCs device architecture. Its inefficiency and lack of stability may significantly restrict the PCE (%) of the device due to low photoelectric conversion [15]. The greater the active surface area of a counter electrode, the more it facilitates rapid catalytic redox activity [16]. The low efficiency of the organic DSSC and the high cost of some of its components are two significant obstacles to its widespread scale-up. The counter electrode is a crucial element that influences this technology's price [15-16]. Platinum-based, carbon-based, and other material-based counter electrodes are the three main varieties generally used in DSSC Solar cell [17]. Among them, the counter electrode in the device assembly using platinum is very costly. Metal materials exhibit outstanding electrical conductivity, good flexibility, exceptional ductility, possesses advanced thermal stability when subjected to high-temperature treatment [18]. Incorporating metal materials as the electrode substrate for solar cells can reduce costs significantly and may enhance solar cell performance by minimizing internal resistance [19]. In order to reduce costs while simultaneously pursuing moderate efficiency, a copper-based counter electrode was employed. The primary aim of this study is to enhance the output electrical performance of DSSCs through the incorporation of an electroplated copper layer in the counter electrode. Furthermore, this study seeks to highlight the potential for cost-effective fabrication of DSSCs by substituting the expensive platinum counter electrode with copper via electroplating.

2. Material and Methodology

2.1 Materials and Chemicals

All the reagents were utilized without being further purified and were procured from commercial sources. Ethanol was used as a solvent to extract a natural dye originating from the Red hibiscus flower collected from the local flower market. For the fabrication of the working electrode, a fluorine-doped tin oxide (FTO) coated on a glass substrate with a surface resistivity of 12–15 Ω sq^{-1} and a thickness of 2.3 mm was acquired from Pilkington (India) and utilized as a conductive surface. The doctor's blade method employed Scotch tape (25 µm thick, Solaronix) to adjust the thickness of the TiO_2 film on the photo anode. On the working electrode, thin film deposition was accomplished using TiO_2 nanoparticle paste (Solaronix, 18 weight percent). PET sheet (2cm x 1cm) was utilized as a base framework for counter electrode fabrication. A graphite pencil (8B) was purchased for the preparation of graphite layer impression on the PET Sheet. Copper (II) sulphate solution (0.5 M, 250 cm^3) was used as a electrolyte for electroplating purposes on the as-prepared PET coated with a graphite counter electrode. Copper strip dimensions (4cm x 2cm) were procured from the local market. The iodide/tri-iodide electrolyte solution was made with potassium iodide and iodine along with HPMC (*Hydroxypropyl methyl cellulose*), which served as a medium for the movement of induced charges between the two electrodes. During device assembly, a 50 µm thick paraffin spacer (Merck, Germany) was utilized as a sealer and a layer of separation between the two electrodes.

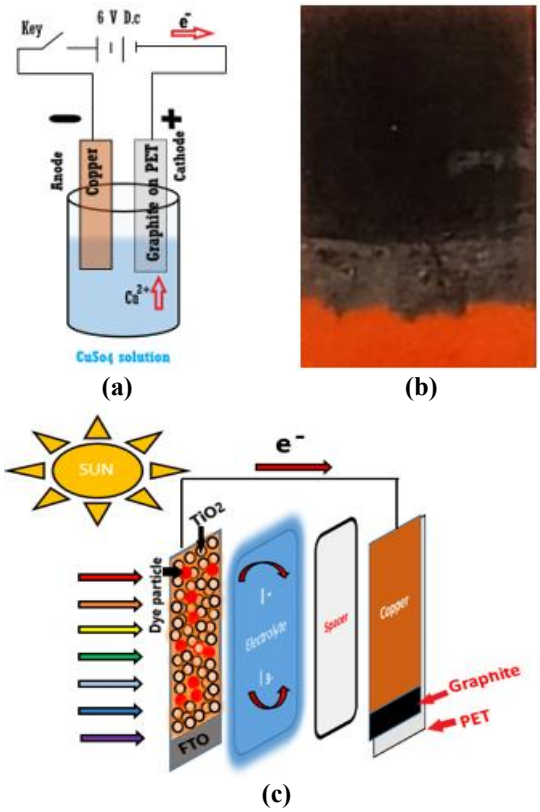

Figure 1: (a) Fabrication scheme of counter electrode via electroplating. **(b)** electroplated copper layer on graphite assisted PET sheet. **(c)** Schematic drawing of the solar cell assembly

2.2 Preparation of Hibiscus flower extracted dye solution

The petals of a fresh hibiscus flower weighing 5 g were cleaned with distilled water and then chopped into little pieces. The flower petals were then pulverized for three minutes in a mixer with 100 millilitres of ethanol. To create a thick solution, the procedure was carried out 5 times. To obtain a uniformly disseminated solution, the mixture was also constantly agitated for one hour using a magnetic stirrer. Before filtering, the solution was stored for 12 hours in a cold, dark environment. Finally, the residue was filtered away and the filtrate dye solution was stored. The dye solution was securely kept in a dark environment at a room temperature 25°C.

2.3 Cleaning of the FTO glass substrate

Prior to TiO_2 deposition, FTO glass substrate was cleaned with distilled water and then ethanol in an ultrasonic bath for ten minutes.

2.4 Photoanode Fabrication

Before material deposition FTO glass substrate was dried properly then the edges of the cleaned FTO glass substrate were covered with scotch tape that was approximately 25 µm thick. Scotch tape was used to restrict the TiO_2 film's thickness to about 25 µm. The doctor blade method was employed for deposition of layer of a transparent TiO_2 nanoparticle paste on

the conducting side of the FTO glass substrate. Before the as prepared TiO_2 film being annealed in a furnace at 480 °C for 45 min, the produced TiO_2 film was dried for about 20 minutes at 60 °C in a hot air oven dryer. Before being dipped in a natural dye solution, the sample was carefully cooled down to prevent any surface flaws or cracks. The as prepared sample was stored at room temperature after being submerged in a dye solution for 24 hours. After gently washing the electrode samples with distilled water to get rid of any excess dye color that hadn't been absorbed. Photo-anode Sample was dried for five minutes at 40 °C in a hot oven air dryer before device assembly.

2.5 Counter electrode preparation

Deionized water was used to create an electrolyte solution with 0.5 M $CuSO_4$ (96%, Sigma-Aldrich), which was then filtered using 0.2-µm filters. The copper plate was cleaned by Ultrasound sonication in isopropanol (99.5%, Sigma-Aldrich) and water in a sequential manner before electroplating. To create a layer of graphite on the PET substrate (2 cm x 1 cm) soft graphite pencil 8B was used. An electrically conductive graphite layer was incorporated by creating an impression on the PET substrate for electroplating purposes. Graphite-assisted PET Counter electrode and Copper metal plate were assembled depicted in the figure 1a, for the electroplating system at room temperature, 25 °C.

2.6 Preparation of electrolyte solution

Here, 100 ml of ethanol was combined with 50 mg of potassium iodide (Sigma-Aldrich, Merck India), 10 mg of iodine and 10 mg of HPMC (Alpha Chemika) in a culture tube, and the mixture was continuously stirred for five minutes. The culture tube holding the electrolyte solution was kept in a dark location.

2.7 Assembling the Solar Cell

The photoanode and the graphite assisted with copper-coated counter electrode were assembled together facing conductive side with each another after being separated by a paraffin spacer (Fig. 1c). Before assembling the device, an electrolyte solution comprising iodide/triiodide (I^-/I_3^-) was injected into the hollow spacer between the counter electrode and working electrode layer. Furthermore, the sandwich-like architecture was fabricated for electrical characterization.

2.8 Characterization

The light absorption characteristics of the dye solution and TiO_2 layer were examined and documented with a UV–Vis spectrophotometer (Hitachi Spectrophotometer, Japan). Field emission scanning electron microscopy (JEOL, Japan) was used to explore the surface topography of the nanostructure on TiO_2 photo-anode and copper counter electrode sample respectively. The diffractogram was analysed with an XRD diffractometer (XPert PRO, USA) using a CuKα radiation source (1.54 Å). Using nickel-filtered CuKα radiation, sources of 40 kV and 30 mA were utilized to measure 2θ in the range of 20°–80°. The performance of the fabricated DSSC was evaluated with an AM 1.5 G sun simulator that provided light irradiation at an intensity of 100 mW cm^{-2} (Compact 150WSolar Simulator, Zolix Instruments, China), using a source meter (model: 2450, Keithley, USA).

3. Results and Discussion

3.1Uv-Vis Analysis

Optical properties of the TiO_2 layer as well as dye solutions were characterized by using an Ultraviolet–visible spectrophotometer (UV–Vis). Figure 2. shows that the light absorption intensity was higher when the dye solution was prepared via the ethanol extraction route.

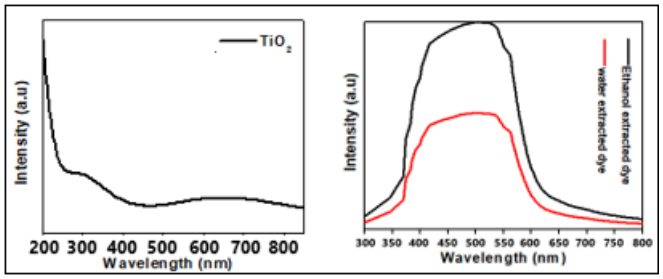

(a) (b)

Figure 2: Optical absorption spectra plot of (a) TiO_2 and (b) dye solutions

The as-prepared ethanolic dye solution shows higher absorption in the 400-600 nm range (visible light region) and a peak observed around 525 nm. The absorption spectra of the TiO_2 film is depicted in Figure a. The maximum absorption range is from 200 nm to 320 nm (ultraviolet region). Optical bandgap was envisaged via the Tauc plot method, and the TiO_2 sample shows an indirect band gap of 3.18 eV.

3.2 Structural analysis

Crystalline structure, phase formation and nature of the fabricated TiO_2 film and Copper electroplated counter electrode were investigated by thin film XRD analysis. Diffraction peaks originating at 2θ =25.78°, 37.6°, 48.06°, 54.37°, 63.2°,75.2° and are corresponding to the lattice planes (101), (004), (200), (211), (204), and (215) confirmed the anatase phase of TiO_2 film. The additional characteristic peaks indicate the presence of the rutile phase mixed with the anatase phase. Diffraction peaks originating at 2θ = 43.1°,50.7°, and 74.4° correspond to the lattice planes (111),(200), and (220), indicating the as-prepared copper film. Sharp and intense peaks in both samples may be ascribed as samples are highly crystalline in nature.

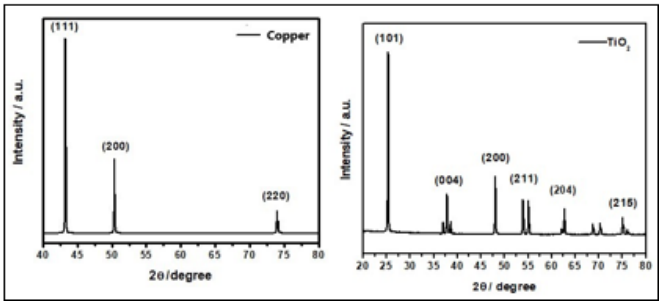

(a) (b)

Figure 3: X-ray diffraction patterns of (a) Copper nanoparticle sample (b) TiO_2

3.3Field Emission Scanning Electron Microscopy Imaging

TiO_2 film and the electroplated Copper sample were characterized by field emission scanning electron microscopy (FESEM) to obtain surface morphology. FESEM image depicted in the fig c shows, almost spherical shape of TiO_2 particle size ~25 nm. Some clusters of TiO_2 particle shows agglomeration due to the presence of rutile along with the anatase phase. Figure a represents the surface morphology of the as-prepared copper film, which has a more compact and uniform particle size than the TiO_2 film. A porous network of TiO_2 helps dye loading, while the surface roughness of the copper counter electrode significantly impacts the electrical performance of the solar cell. Several cracks were observed on the graphite layer in fig b due to induced strain. Strain-induced surface cracks minimize the surface area of the conductive path. Conductive layer of copper on the graphite helps in reduction of void space on the film, substantially reducing the recombination rate of electron hole pair, concomitantly improving the PCE of the solar cell.

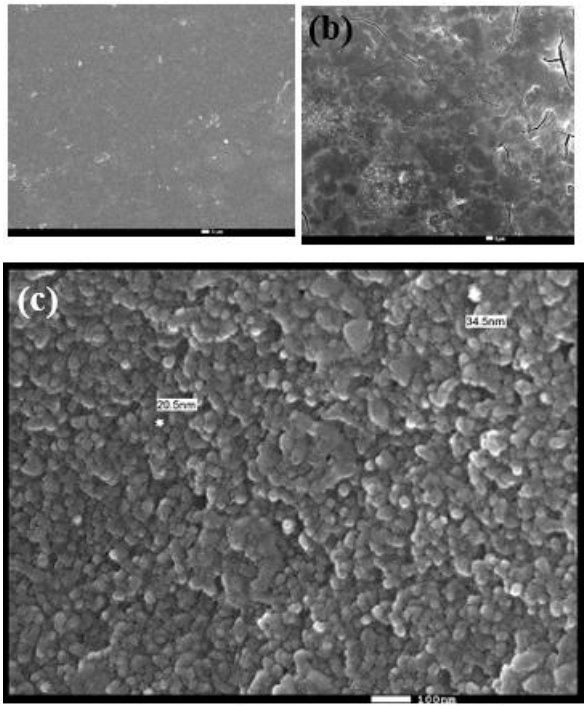

Figure 4: FE-SEM images of surface topography of prepared (**a)** Copper layer (**b)** graphite layer (**c**)TiO_2 layer on PET sheet

3.4 Energy dispersive X-ray Spectroscopy(EDS)

Quantitative elemental analyses of the as-prepared coatings were investigated via EDS characterisation technique. Elemental map scanning was carried out for both samples during EDS sample characterisation, and the results were depicted in fig 5. Figure a exhibits a prominent characteristic peak originating at 4.5eV confirms the presence of Titanium. Typical EDS pattern depicted in fig b exhibits for the copper-coated sample possesses a low stoichiometric ratio of elemental copper. The surface analyses conducted via EDS confirm the homogeneity of the samples as the stoichiometric ratio are consistent for both the samples.

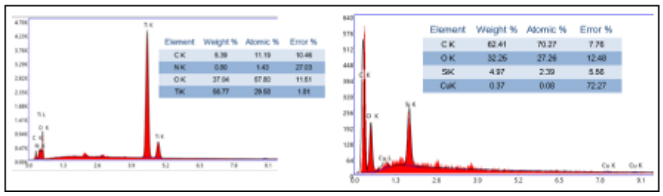

(a) (b)

Figure 5 EDS data of (a)TiO_2 (b) Electroplated Copper layer of graphite assisted PET sheet

3.5 PhotoVoltaic Characterization

The photovoltaic performance of the DSSC samples was tested under an AM 1.5G optical filter, and subsequently, current density versus voltage (J–V) curves were analyzed. Light illumination was kept at 100 mW $cm^{-2,}$ and data were recorded at room temperature, 20°C. Photovoltaic parameters open-circuit voltage (V_{oc}), short circuit current density (J_{sc}), fill factor (FF), and efficiency (η) are depicted in table no1.

Table 1: Photovoltaic parameters of Copper incorporated and devoid of copper layer in the counter electrode in DSSC cells (active area of cell was 1 cm^2)

Counter Electrode	VOC (V)	JSC (mA/cm^2)	FF (%)	η (%)	RSh Ohm. cm^2	RS Ohm. cm^2
1.Without Cu layer	0.45	9.88	45	2	454.5	384.6
2.With Cu layer	0.60	9.09	55	3	1250	27.78

Data reveals that a device assembled with copper as a layer in the counter electrode exhibits higher PCE (%). Increase open circuit voltage, fill factor, as well as power conversion efficiency in the copper assembled counter electrode possibly due to the defect reduction in the counter electrode via electroplating. Higher V_{OC} offers a slow recombination rate. Series resistance of the samples shows that modification in the counter electrode reduces charge transfer resistance, as a result fill factor improved. The highest PCE was observed 3% in the DSSC sample have copper in the counter electrode, which is comparative 150% higher than the sample without a copper layer in the sample.

.

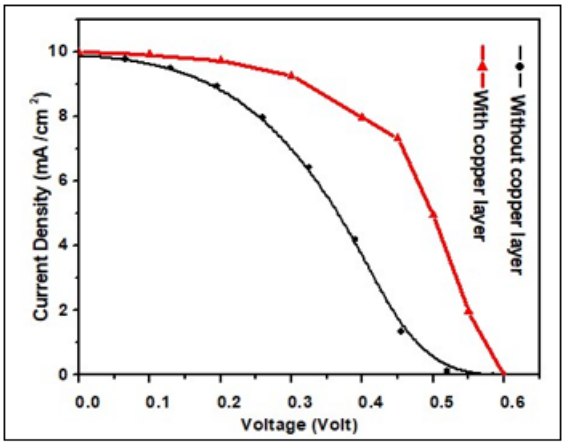

Figure 6: Current density–voltage (J–V) plots of DSSC solar cell sample devoid of copper layer and incorporated copper layer in the counter electrode

3.6 Static Contact Angle measurement

Surface homogeneity of the as-prepared counter electrode was analyzed using the static contact angle measurement technique. A drop of water was placed on the active side of the counter electrode, and subsequently, static images were captured via a camera kept stationary on the surface. When the liquid is released from the static droplet and the base of the counter electrode makes 0° with the horizontal plane, the baseline remains stable in a static position. The adhesion condition of the droplet on the electrode surface was explored via tilting angle measurement. The contact angle was estimated from the captured images using software based on a suitable curve-fitting method. Advancing contact angle (ACA) and receding contact angle (RCA) were estimated approximately 64.729° and 60.098°, respectively, while the electrode sample was tilted at approximately 35.08° (sliding angle) with the horizontal surface. Minimal change between ACA and RCA indicates low contact angle hysteresis.

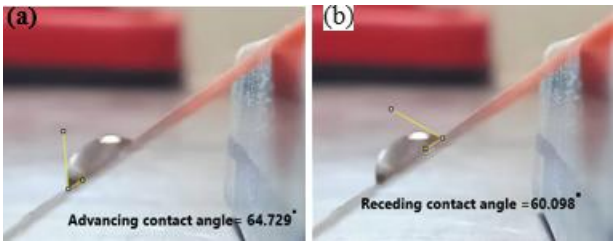

(a) (b)

Figure 7: Liquid droplet is in contact with the as prepared copper coated counter electrode surface **a**. advancing contact angle **b.** receding contact angle.

3.7 Relative conductivity measurement

The electrical conductivity of the deposited material is largely influenced by the Electroplating time, as the deposited material thickness increases with electroplating time. Fig. 8 depicts relative conductivity vs. electroplating time for the as-prepared copper layer on a graphite-coated PET sheet.

Electroplating time up to 10 min shows a continuous increment of the conductivity, which may be ascribed to a thin and continuous coating of copper layer on graphite. Electroplating time more than 10 minutes shows the rate of increase of electrical conductivity is minimized. This can be attributed to the irregular accumulation of copper particles on the thin films, which forms a secondary structure on the thin film. Electroplating time beyond 25 minutes results in a decrease in electrical conductivity, as prolonged electroplating Causes irregular agglomeration of copper ions on the thin film, which might increase the surface resistivity.

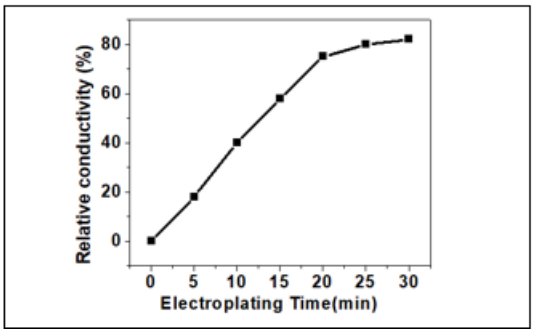

Figure 8: Variation of sheet resistance with the change of thickness of the electroplated copper layer

4. Conclusion

The counter electrode extracts electrons efficiently from the electron-hole pair and returns them to the cell, establishing a complete circuit. The sintered TiO_2 sample exhibits almost uniform spherical particle size that may help with dye loading. An electroplated copper layer on the PET coated with graphite impressively improves the surface smoothness. The PET sheet devoid of a copper layer possesses several cracks

On the graphite layer, which might reduce the charge transport rate. It has been found that the surface resistance affects the efficiency of the solar cell; a low series resistance improves efficiency, whereas a high shunt resistance suppresses the recombination rate. Higher open circuit voltage, along with lower series resistance, offers a lower recombination rate and improves the fill factor when a copper layer is incorporated on the graphite layer. Lower contact angle hysteresis may be attributed to a uniform smooth surface. Due to its high charge transport rate, platinum is the most widely utilized electrode in DSSCs; however, because of its high price, scalable production is not possible. Copper is abundantly available, which is being employed instead.

An attempt was made to replace the costly platinum counter electrode in DSSC with Copper.

Conflicts of interest There are no conflicts to declare**.**

Funding The authors received no specific funding for this work.

Ethics: not applicable

Consent to Participate not applicable

Consent to Publish declarations not applicable

Data availability

The authors declare that all data generated or analysed during this study are included in this published article [and its supplementary information files].The datasets generated during and/or analysed during the current study are available from the corresponding author on reasonable request.

References

[1] K. V. Srivastava, P. Srivastava, A. Srivastava, R. K. Maurya, Y. P. Singh, and A. Srivastava, “1D TiO 2

photoanodes: a game-changer for high-efficiency dye-sensitized solar cells," RSC Adv., vol. 15, no. 7, pp. 4789–4819, 2025, doi: 10.1039/d4ra06254j.
[2] S. Xu et al., "Renewable flower-based dye-sensitized solar cells using natural dye and natural carbon counter electrode," Energy Adv., vol. 4, no. 7, pp. 947–957, 2025, doi: 10.1039/d5ya00086f.
[3] N. Al-Shamery et al., "From black pigment to green energy: shedding light on melanin electrochemistry in dye-sensitized solar cells," Mater. Adv., vol. 6, no. 10, pp. 3073–3083, 2025, doi: 10.1039/d5ma00081e.
[4] M. Kokkonen et al., "Advanced research trends in dye-sensitized solar cells," J. Mater. Chem. A, vol. 9, no. 17, pp. 10527–10545, 2021, doi: 10.1039/d1ta00690h.
[5] M. A. Marsya, S. Lee, G. M. Alvien, I. N. P. Permanasari, K. Choi, and J. Hong, "Highly transparent dye-sensitized solar cells with UV-absorbing fluorene dyes and tetramethylthiourea electrolytes," Sci Rep, vol. 15, no. 1, Dec. 2025, doi: 10.1038/s41598-025-89486-z.
[6] A. Daniel and J. H. Delcamp, "Dye-Sensitized Solar Cells: A Brief Historical Perspective and Uses in Multijunction Devices," Challenges and Advances in Computational Chemistry and Physics. Springer International Publishing, pp. 81–98, 2021. doi: 10.1007/978-3-030-69445-6_4
[7] S. A. Badawy, E. Abdel-Latif, and M. R. Elmorsy, "Tandem dye-sensitized solar cells achieve 12.89% efficiency using novel organic sensitizers," Sci Rep, vol. 14, no. 1, Oct. 2024, doi: 10.1038/s41598-024-75959-0.
[8] A. Subhan, K. Dharmalingam, A.-H. I. Mourad, S. T. Mahmoud, and H. Alawadhi, "Improved photovoltaic performance of dye-sensitized solar cell upon doping with pulsed-laser fabricated plasmonic silver nanoparticles as modified photoanodes," Mater Renew Sustain Energy, vol. 14, no. 2, Jun. 2025, doi: 10.1007/s40243-025-00315-9.
[9] N. Y. A. Azmi, A. N. Efandi, N. A. S. Aziz, L. Roza, E. R. Mawarnis, and M. Y. A. Rahman, "Review on metal, binary and ternary alloy as counter electrode for dye-sensitized solar cells," J Mater Sci: Mater Electron, vol. 36, no. 17, Jun. 2025, doi: 10.1007/s10854-025-15100-7.
[10] N. Al-Shamery et al., "From black pigment to green energy: shedding light on melanin electrochemistry in dye-sensitized solar cells," Mater. Adv., vol. 6, no. 10, pp. 3073–3083, 2025, doi: 10.1039/d5ma00081e.
[11] O. I. Francis and A. Ikenna, "Review of Dye-Sensitized Solar Cell (DSSCs) Development," NS, vol. 13, no. 12, pp. 496–509, 2021, doi: 10.4236/ns.2021.1312043.
[12] S. Qamar and S. Erten Ela, "Dye-sensitized solar cells (DSSC): Principles, materials and working mechanism," Current Opinion in Colloid & Interface Science, vol. 74, p. 101871, Dec. 2024, doi: 10.1016/j.cocis.2024.101871.
[13] V. Yadav, Y. Soni, C. M. S. Negi, S. K. Gupta, and U. Kumar, "Role of natural dye in photovoltaic performance of dye-sensitized solar cell," Materials Today: Proceedings, vol. 68, pp. 2781–2784, 2022, doi: 10.1016/j.matpr.2022.09.483.
[14] S. Rahman et al., "Research on dye sensitized solar cells: recent advancement toward the various constituents of dye sensitized solar cells for efficiency enhancement and future prospects," RSC Adv., vol. 13, no. 28, pp. 19508–19529, 2023, doi: 10.1039/d3ra00903c.
[15] K. Prajapat et al., "Next-generation counter electrodes for dye-sensitized solar cells: A comprehensive overview," Sustainable Materials and Technologies, vol. 42, p. e01178, Dec. 2024, doi: 10.1016/j.susmat.2024.e01178.
[16] S. C. Yadav, A. Sharma, R. S. Devan, and P. M. Shirage, "Role of different counter electrodes on performance of TiO2 based dye-sensitized solar cell (DSSC) fabricated with dye extracted from Hibiscus Sabdariffa as sensitizer," Optical Materials, vol. 124, p. 112066, Feb. 2022, doi: 10.1016/j.optmat.2022.112066.
[17] S. Ding, C. Yang, J. Yuan, H. Li, X. Yuan, and M. Li, "An overview of the preparation and application of counter electrodes for DSSCs," RSC Adv., vol. 13, no. 18, pp. 12309–12319, 2023, doi: 10.1039/d3ra00926b.
[18] S. R. Raga and F. Fabregat-Santiago, "Temperature effects in dye-sensitized solar cells," Phys. Chem. Chem. Phys., vol. 15, no. 7, p. 2328, 2013, doi: 10.1039/c2cp43220j.
[19] M. M. Hasan and N. K. Allam, "An alternative, low-dissolution counter electrode to prevent deceptive enhancement of HER overpotential," Sci Rep, vol. 12, no. 1, Jun. 2022, doi: 10.1038/s41598-022-13385-w.